Edited by H. Ryssel, P. Pichler - September 1995

Large Signal Frequency Domain Device Analysis Via the Harmonic Balance Technique

B. Troyanovsky, Z. Yu, and R. W. Dutton

Center for Integrated Systems,
Stanford University,
Stanford, CA 94305, USA

Abstract

Harmonic and intermodulation distortion effects play a key role in the design and subsequent performance of analog RF/μWave systems. Due to the wide range of frequency components present in such systems, ordinary transient analysis is both extremely time-consuming and insufficiently accurate. In this paper, we present a harmonic balance version of the PISCES semiconductor device simulator. This two-dimensional device simulation tool allows for efficient, physically-based analysis of intermodulation distortion in two-dimensional device structures. Robust nonlinear relaxation methods have been developed to overcome the enormous memory and speed problems associated with fully-coupled, large-signal 2D frequency-domain analyses.

1. Introduction

Harmonic balance (HB) is a nonlinear frequency domain analysis technique which is widely used to simulate harmonic/intermodulation distortion in nonlinear high-frequency circuits [1] [2]. However, current frequency domain (HB) tools are circuit simulators which require lumped (or analytic) models for the active devices. Such models are not based on numerical solution of the semiconductor equations, and as a consequence are not predictive. They require the active semiconductor components to be characterized in advance and fit to a lumped equivalent model.

We have developed a harmonic balance version of the PISCES [3] device simulator to address the above concerns. This two-dimensional HB device simulation tool solves the drift-diffusion system of semiconductor equations in the frequency domain, using the full complement of standard PISCES physical models. A given simulation run yields the spectra corresponding to terminal current/voltage, as well as internal device potential and carrier concentrations, based on a large signal quasi-periodic input. The effects of external packaging and parasitics are handled through a mixed level circuit/device capability which supports linear elements characterized via S-parameters.

To underscore the advantages of a harmonic balance approach when the device is driven by a combination of sinusoids, we examine a typical two-tone input used for intermodulation distortion tests. The driving voltages for such tests have the form $V_{IM} = A\cos(\omega_a t + \phi_a) + B\cos(\omega_b t + \phi_b)$, where the frequencies ω_a and ω_b are closely spaced. For infinitesimally small amplitudes A and B, the device will behave linearly, and the system will respond only at the frequencies ω_a and ω_b. However, as the amplitudes increase, the nonlinearities within the system will give rise to distortion components. In general, the frequencies present in the response will then be given by the set

$$\omega_{k_1 k_2} = k_1\omega_a + k_2\omega_b \geq 0, \tag{1}$$

where k_1 and k_2 are integers. The close spacing of ω_a and ω_b results in some frequency components (such as $\omega_a - \omega_b$) which are many orders of magnitude smaller than those in the two-tone input. For example, if $f_a = 1GHz$ and $f_b = 1GHz - 30kHz$ (with $f_a - f_b = 30kHz$), an accurate transient analysis involves integrating over at least 10^5 periods of the high-frequency sinusoid, with spacing fine enough to resolve its harmonics. Further complications arise due to the slow decay of transients, and the relatively poor accuracy with which low-amplitude harmonics are resolved in low-distortion systems.

2. Applying Harmonic Balance to the Time-Dependent Semiconductor Equations

The harmonic balance algorithm overcomes these shortcomings by solving the problem in the frequency domain, and thus avoiding time discretization altogether. PISCES solves the drift-diffusion equations

$$\begin{aligned} \nabla\cdot(-\epsilon\psi) &= q(p - n + N_D^+ - N_A^-) && (2)\\ \frac{\partial n}{\partial t} &= \frac{1}{q}\nabla\cdot J_n - U && (3)\\ \frac{\partial p}{\partial t} &= -\frac{1}{q}\nabla\cdot J_p - U && (4) \end{aligned}$$

where in addition we have the auxiliary relations $J_n = qD_n\nabla n - q\mu_n n\nabla\psi$ and $J_p = -qD_p\nabla p - q\mu_p p\nabla\psi$. For transient analysis, these equations are discretized in both time and space, and the basic variables at each internal node k (ψ_k, n_k, p_k), along with voltages (v_q) at appropriate external nodes q, are solved for at each time step via an implicit integration scheme. The HB version of the code retains the space discretization, but assumes that the basic variables (ψ_k, n_k, p_k, v_q) have the form

$$x_n(t) = x_{n0} + \sum_{h=1}^{H} x_{nh}\cos(\omega_h t) + x_{n,h+H}\sin(\omega_h t) \tag{5}$$

where $\mathbf{x} = [\psi_1\ n_1\ p_1\ \psi_2\ n_2\ p_2\ \cdots\ \psi_K\ n_K\ p_K\ v_1\ v_2\ \cdots v_Q]^T$, K is the number of internal grid nodes, Q is the number of external circuit nodes, H is the number of harmonics used in the analysis, and $1 \leq n \leq 3K + Q$. The frequencies ω_h represent a finite subset of (1) and need not be harmonically related.

If we substitute (5) into (2) - (4) and discretize in space, we obtain a time-domain system of the form

$$F_n(t) = \delta_{cont} x_n'(t) + G_n(\mathbf{x}(t)) \to 0 \tag{6}$$

where $1 \leq n \leq 3K$, and δ_{cont} is unity for the continuity equations while being zero for the Poisson equation. The goal of the harmonic balance analysis is to determine the set of coefficients x_{nh} in (5) such that (6) is satisfied, along with the auxiliary KCL equations for the external linear elements.

Given a guess for the harmonic coefficients x_{nh}, we can sample the residual functions $F_n(t)$ at $2H + 1$ appropriate time instants to obtain the residual quasi-Fourier coefficients via a matrix transformation analogous to the DFT [1]. That is, we compute the coefficients F_{nh} such that $F_n(t) = F_{n0} + \sum_{h=1}^{H} F_{nh}\cos(\omega_h t) + F_{n,h+H}\sin(\omega_h t)$. Thus, the harmonic residual coefficients F_{nh} can be viewed as functions of the unknowns x_{nh}. If we let $\boldsymbol{\theta}$ denote the $(3K+Q)(2H+1)\times 1$ vector of coefficients x_{nh}, and if we let $\boldsymbol{\Phi}$ denote the corresponding vector of F_{nh}, we end up with a $(3K+Q)(2H+1)\times(3K+Q)(2H+1)$ nonlinear system of the form

$$\boldsymbol{\Phi}(\boldsymbol{\theta}) \rightarrow \mathbf{0} \tag{7}$$

The Jacobian of (7) may be evaluated via straightforward application of the chain rule, and the system may then be solved using standard nonlinear solution techniques.

3. Nonlinear Relaxation Methods

Solving the harmonic balance equations with the fully-coupled direct Newton method is prohibitively expensive, as the memory needed to factor the Jacobian scales as $(2H+1)^2$ with the number of harmonics. Thus, even a modest analysis at 10 harmonics would require 441 times as much memory as a PISCES DC analysis.

Consequently, we utilize a modified block Gauss-Seidel-Newton nonlinear relaxation scheme [4] to solve (7). We define spectral error norms at each harmonic $0 \leq h \leq H$ as follows

$$e_h = \sum_{n=1}^{3K+Q} \left(|F_{nh}| + (1-\delta_h)\,|F_{n,h+H}|\right) \tag{8}$$

where δ_h is unity for $h = 0$, and zero otherwise. The nonlinear relaxation scheme proceeds by starting from an initial guess, which is typically a PISCES DC solution. On a given iteration, all harmonics except the one with the highest error norm are held fixed, while a single Newton step is performed on the subset corresponding to the highest e_h. The process is repeated until all error norms fall below a specified tolerance. We see that this algorithm requires only four times as much memory as a DC analysis, regardless of the number of harmonics H.

The aforementioned algorithm is guaranteed to converge at low drive levels, since in this case the harmonics decouple and the relaxation scheme reduces to a sequence of linear AC analyses. Experience has shown that the algorithm continues to exhibit extremely robust convergence in virtually all situations of practical interest when it is applied to the semiconductor equations. In addition, it offers a speed of convergence which is typically over an order of magnitude faster than that of fully-coupled Newton.

4. Examples

In this section, we present harmonic balance PISCES analyses of a high-performance silicon npn-BJT [5]. A cross-section of the device is illustrated in Fig. 1. Fig. 2 and Fig. 3 illustrate the collector current response in the frequency- and time-domain, respectively, when the device is driven by $V_{be} = 0.65 + 0.1\sin(10^{10}t)V$, $V_{ce} = 2.0V$. This harmonic balance run took slightly under an hour of simulation time on an HP-735 workstation.

Fig. 4 shows the results of a two-tone intermodulation distortion analysis carried out at 24 harmonics. The input to the BJT is $V_{be} = 0.65 + 0.02(\sin(10^8 t) + \sin(10^7 t))$, $V_{ce} = 2.0V$, with the analysis taking 3hr. 15min. High levels of intermodulation distortion are present in the collector current spectrum.

References

[1] K.S. Kundert, J.K. White, and A. Sangiovanni-Vincentelli, *Steady-State Methods for Simulating Analog and Microwave Circuits*, Kluwer Academic Publishers, 1990

[2] V. Rizzoli and A. Neri, "State of the art and present trends in nonlinear microwave CAD techniques," IEEE Trans. on Microwave Theory and Techniques, pp.343-365, Feb. 1988

[3] Z. Yu, D. Chen, L. So, and R.W. Dutton, *PISCES-2ET — Two-Dimensional Device Simulation for Silicon And Heterostructures*, Stanford University, 1994

[4] J. Ortega and W. Rheinboldt, *Iterative Solution of Nonlinear Equations in Several Variables*, Academic Press, 1970

[5] P. Vande Voorde, D. Pettengill, and S.Y. Oh, "Hybrid simulation and sensitivity analysis for advanced bipolar device design and process development," IEEE 1990 Bipolar Circuits and Technology Meeting, Minneapolis, Minnesota

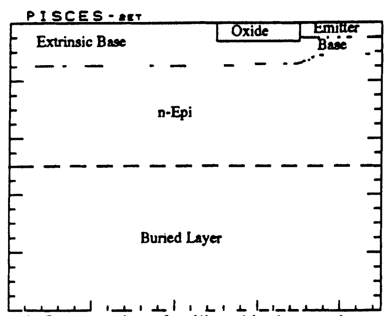

Figure 1. Cross-section of a silicon bipolar transistor used for harmonic balance PISCES analysis.

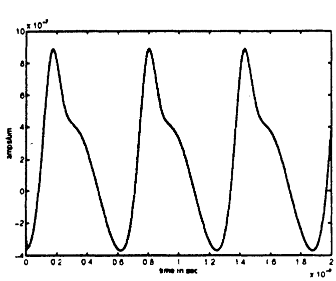

Figure 3. Time-domain representation of Figure 2. The harmonic balance run is drawn as a solid line, whereas a PISCES transient run is drawn dashed. No difference between the two can be seen.

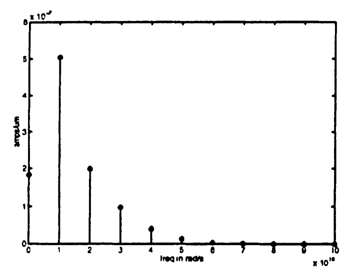

Figure 2. Collector current spectrum under a large-signal single-tone sinusoidal input.

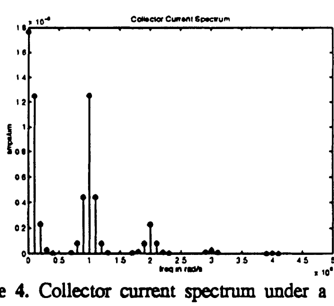

Figure 4. Collector current spectrum under a two-tone intermodulation distortion test.